PERGAMON

International Journal of Multiphase Flow 27 (2001) 561–570

International Journal of Multiphase Flow

www.elsevier.com/locate/ijmulflow

Brief communication

Taylor bubbles in miniaturized circular and noncircular channels

Q.C. Bi, T.S. Zhao*

Department of Mechanical Engineering, The Hong Kong University of Science and Technology, Clear Water Bay, Kowloon, Hong Kong

Received 19 November 1999; received in revised form 15 March 2000

1. Introduction

The study of two-phase flow and boiling heat transfer in a confined space or micro-sized geometry has received considerable attention in the past few years because of its applications in the cooling of a wide variety of devices, such as high-density multi-chip modules in supercomputers, high-heat-flux modular electronics, high-powered X-ray and other diagnostic devices, high-flux heat exchangers in aerospace systems, cryogenic cooling systems in satellites, and so on. One of the important aspects associated with two-phase flows in microchannels is to study the bubble behaviors. In this work, the motion of elongated bubbles formed in miniature channels with stagnant liquids is investigated.

Drift-flux model is widely used for the analysis of gas–liquid two-phase flows, primarily because it is applicable to various flow patterns and a wide range of void fractions. According to the theory (Wallis, 1969), the velocity of the gas phase in a tube is given by

$$v_G = j_G/\epsilon = C_0 j + V_b \tag{1}$$

where ϵ is the void fraction, C_0 is the distribution parameter, and $j = (j_L + j_G))$ represents the mixture volumetric flux with j_L and j_G being the superficial velocities of liquid and gas phase. The last term V_b in Eq. (1) is the so-called drift velocity, which is defined as the velocity of penetration of a bubble into a stagnant liquid column, as the liquid is emptied from the tube

* Coresponding author. Tel.: +852-2358-8647; fax: +852-2358-1543.
E-mail address: metzhao@ust.hk (T.S. Zhao).

PII: S0301-9322(00)00027-6

(Benjamin, 1968). Generally, the drift velocity is influenced by various forces exerted on the bubble, such as the local interfacial drag, the buoyancy force, and the surface tension.

Previous studies (Zukoski, 1966; Tung and Parlange, 1976; Kataoka et al., 1987) have shown that the bubble rising velocity in vertical tubes with large diameters is proportional to $\sqrt{gd}$, where g is the local gravitational acceleration and d is the tube diameter. It has also been shown that when the tube size is sufficiently small, the bubble rising velocity diminishes faster than $\sqrt{d}$, and for tubes of small enough diameter, bubble motion in the stagnant water ceases completely.

It should be noted, however, that the above conclusions concerning the drift velocity were drawn based on the experiments in circular tubes. Recently, a new type of ultracompact condenser consisting of a number of parallel, multiport miniaturized non-circular channels with hydraulic diameter of 0.3 mm $\leq D_h \leq$ 2.0 mm has been developed (Guntly and Costello, 1991). Although this ultracompact condenser appears to be a promising heat exchanger for a wide variety of engineering applications, there is virtually no research work performed on two-phase flows in these miniaturized non-circular tubes. For instance, the bubble rising behaviors in miniaturized triangular or rectangular tubes remain unclear. Motivated by this need, we have experimentally investigated the elongated bubble behaviors in miniature noncircular channels. The experiments showed that for the triangular and rectangular channels, elongated bubbles always rose upward even though the hydraulic diameter of the tube was as small as 0.866 mm. This unique phenomenon is reported for the first time in this paper.

2. Experimental apparatus

The experiments were carried out in a number of the test sections including eleven circular tubes, three triangular channels, two square channels, and one rectangular channel. The three circular test sections with large diameters (6.35, 4.36, and 3.18 mm) were made from Tygon® tubing, whereas the others having diameters of 2.89, 2.78, 2.70, 2.58, 2.50, 2.32, 2.17, and 1.89 mm were fabricated using Lucite glass. These circular tubes had a length of 200 mm. As shown in Fig. 1a, the three larger circular tubes were tested by inserting in a slender water container with a rectangular cross-section so that the influence of the light refraction by the curved surface of the tubes on the results of flow visualization could be minimized. All the noncircular channels were made from Lucite glass. The side lengths of the three triangular channels (shown in Fig. 1b) were 5.0, 2.5, and 1.5 mm, which are equivalent to 2.886, 1.443, and 0.866 mm in hydraulic diameter. The two square channels had side lengths of 1.5 and 1.0 mm (1.5 and 1.0 mm in hydraulic diameter), whereas the rectangular channel had (shown in Fig. 1c) a cross-section of 1.5×0.75 mm^2 (1.0 mm in hydraulic diameters). All the noncircular channels tested had a length of 270 mm. Air bubbles were injected into the test sections by a gas nozzle (a capillary glass pipette with an inner diameter of 0.556 mm), which was located at the bottom of test sections and connected to a vibrating orifice aerosol generator (TSI Model 3450) through Tygon® tubing. One of the most important features of this aerosol generator (used to inject air into water) is that the air injector can be pushed at an extremely slow speed ranging from 0.1×10^{-3} to 9.9×10^{-2} mm/s. In the present experiment, an injector having a cross-sectional area of 5.5×10^2 mm^2 was used. In order to minimize the influence of the injection

on the bubble departure behaviors, the injecting speed was set at as low as 0.5×10^{-2} mm/s. All the experiments were performed by keeping the nozzleat at a location 240 mm below the water level.

A high-speed motion analyzer (Kodak Ekapro-1000) was employed to visualize the bubble behaviors in the test sections. The bubble behaviors were observed by analyzing the images taken at a speed of 1000 pictures per second for full screen or up to 12,000 pictures per second for split screen and replayed at a speed as slow as one picture per second afterwards. In addition, a digital handy video camera (Sony DCR-TRV900E) was also used in the test. A Nikon 105 mm telephoto lens and Nikon bellows PB-6 were used for micro shooting. The bubble rising velocity was determined by the image processing toolbox of a commercial software MATLAB based on measuring the position change of the gas slug tail in terms of the image pixels in the consecutive frames recorded by the high-speed camera.

3. Visualization results and discussion

In order to show how tube walls affect bubble behaviors, and examine the measuring accuracy of the test setup, we first performed the experiments on the bubble departure characteristics in an open water pool in which bubbles were injected from the nozzle located at

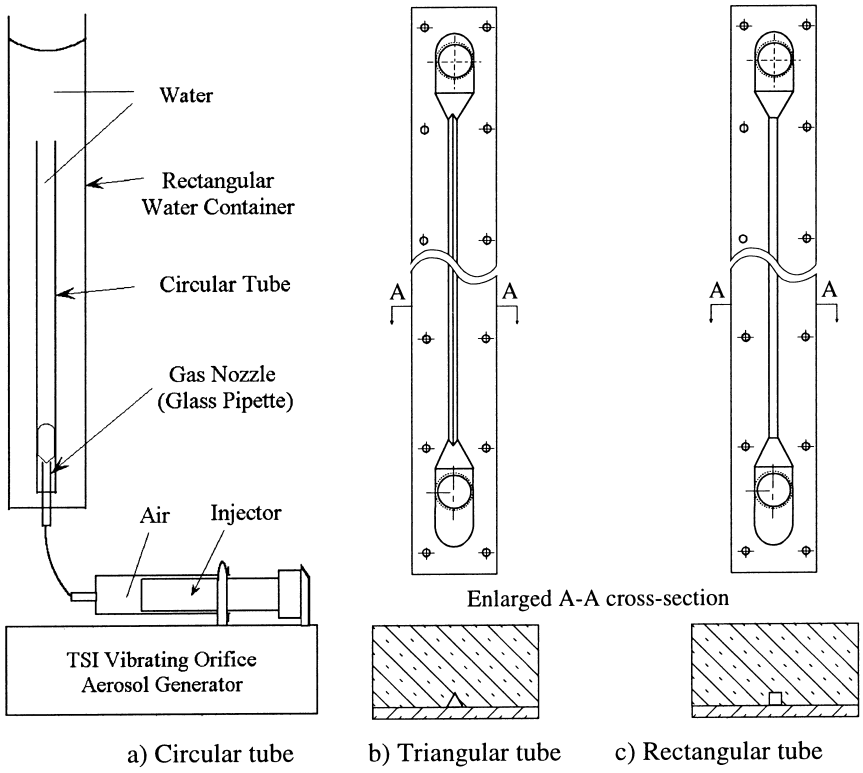

Fig. 1. Schematic diagram of the test sections.

the bottom. Consecutive snapshots of typical bubble formation, growth, and departure from the nozzle are presented in Fig. 2a. It is seen from this figure that as the air pressure in the nozzle became sufficiently high, a tiny air bubble appeared (see the second image) taking the shape of a nearly perfect sphere. As seen from the third to the sixth image, once formed, the air bubble grew up and was elongated in the vertical direction due to the effect of the buoyancy force. As the size of the bubble became large enough, the neck linking the bubble to the nozzle became extremely thin. Immediately following this instant, the bubble departed from the nozzle and rose up. As indicated in the seventh image of Fig. 2a, at the instant of bubble departure, its diameter was 2.67 mm, which was measured along the horizontal direction (departure diameter is 2.84 mm, which is the volume-equivalent sphere diameter). The bubble horizontal diameter was increased to 2.73, 2.99 and 3.17 mm afterwards because of its deformation. Theoretically, the departure diameter of a bubble in an open water pool when gas is injected through an orifice can be predicted by an equation given by Wallis (1969)

$$d_b = 2\left[\frac{\sigma \cdot R_o}{g \cdot (\rho_L - \rho_G)}\right]^{1/3} \tag{2}$$

where σ is the surface tension of water, R_o is the radius of the gas nozzle, ρ_L and ρ_G represent the densities of water and air, respectively. Based on Eq. (2), the bubble departure diameter is 2.9 mm under the condition of 25°C and 1 bar. Apparently, this value is in reasonable agreement with the present experimental data ($d_b = 2.84$ mm).

We now present the results of the visual study on the bubble behaviors in the circular tubes closed at the bottom. Fig. 2b shows the bubble behaviors in the tube of $d = 3.18$ mm. It is seen that at the instant of bubble departure (the fifth image in Fig. 2b), the bubble horizontal diameter was 2.70 mm (the volume-equivalent sphere diameter $d_b = 2.78$ mm), which is rather close to the value predicted by Eq. (2) for the case of the open water pool discussed above, implying that the tube wall has no effect on the bubble departure diameter. This is because at the instant of bubble departure the smaller bubble was mainly influenced by the buoyancy force and the surface tension between the bubble and the nozzle. However, it was observed that once a bubble departed from the nozzle, the tube wall had an influence on the bubble behavior, reflected by the slower rising velocity as compared with the case of the open pool, even though the bubble kept rising in the tube. The experimental results for the large-diameter tubes ($d = 6.35$ and 4.36 mm) also indicate that the bubble departure diameter in the tubes was not affected by the tube wall, but the rising velocities in the large-diameter tubes became higher than those in the tube of $d = 3.18$ mm.

However, as the diameter of the tube became smaller, the air bubble in the tube behaved differently. First of all, the drift velocity was found to become smaller with the decrease in the tube diameters. It was further observed that the up-motion of gas slugs ceased completely when the diameter of the circular tubes was reduced to a value less than the bubble departure diameter predicted by Eq. (2), i.e.: $d = 2.9$ mm. In the tubes with diameters $d = 2.89$ mm and $d = 2.78$ mm, the gas plug formed and this can be evident from the consecutive snapshots of the bubble behaviors in the tube of $d = 2.78$ mm presented in Fig. 2c. As seen from the figure, bubbles usually departed from the nozzle and rose up in the tube with the critical diameter. However, since the departed bubble was deformed during its rising along a spiral path, it

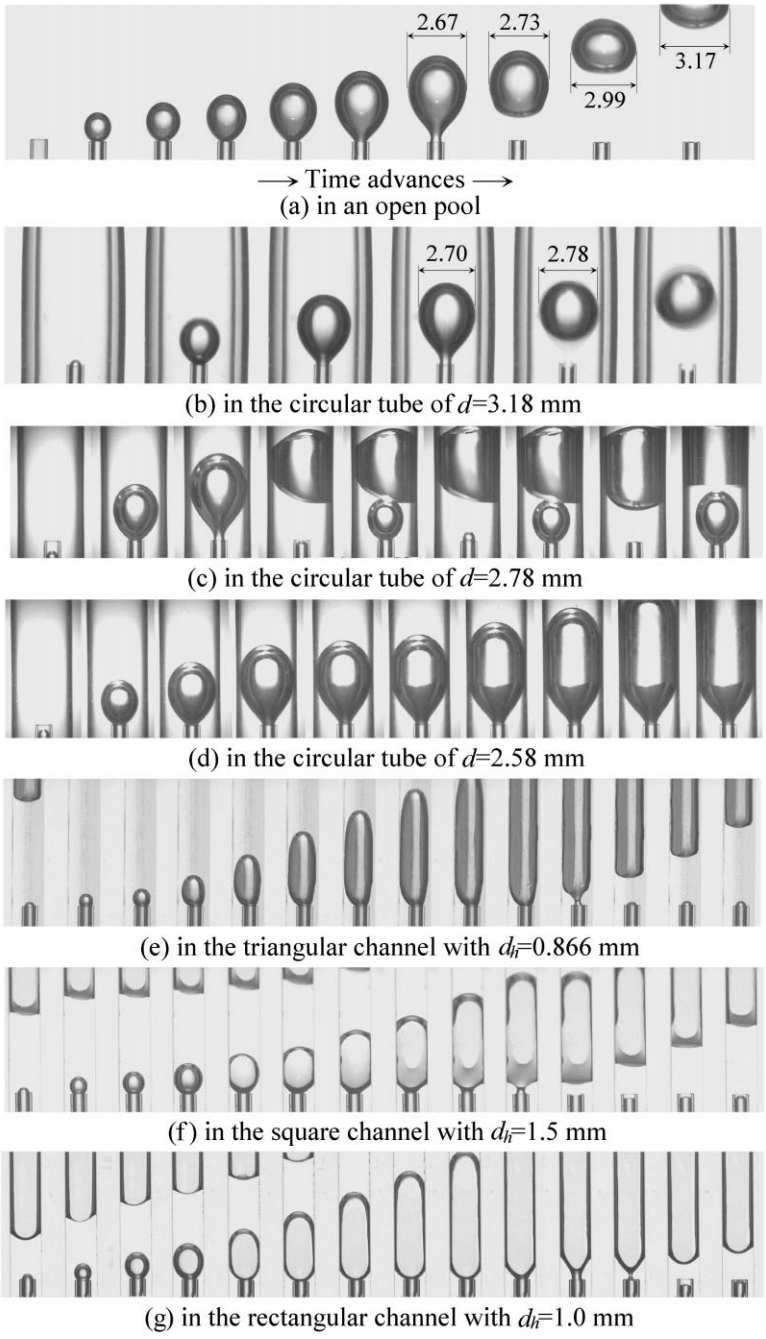

Fig. 2. The images of the bubble behaviors as time advanced.

adhered to the tube wall at a certain elevation due to relatively large surface tension for a small-diameter tube. The bubble adhered to the tube wall grew up due to the collision and coalesced with the subsequent departed bubbles. As a result, a gas plug formed within the tube. Since the gas plug separated the liquid column in the tube and the liquid phase became discontinuous, the buoyancy force played no role in assisting the air plug in rising and its motion ceased completely, meaning that the drift velocity was zero.

When the tube diameter was smaller than 2.78 mm, it was found that the bubble never departed from the nozzle. Typical situations are shown in Fig. 2d for the tube of $d = 2.58$ mm. The second to the fourth images in Fig. 2d indicate that initially the air bubble grew up by pushing the surrounding water. Further bubble growth was restricted by the tube wall (see the fifth image of Fig. 2d). The subsequent addition of air caused the growth of the gas slug in the vertical direction only, and as a result, a gas plug formed (see the last image of Fig. 2d). As mentioned earlier, once a gas plug had formed, the liquid column became discontinuous and the buoyancy force vanished. Thus, the gas plug never departed from the nozzle and never rose in the tube. Similar situations were observed for the circular tubes with diameter less than 2.58 mm.

Next, we turn our attention to Fig. 2e, where the gas bubble behaviors in the vertical capillary triangular channels ($d_h = 0.866$ mm) closed at the bottom are presented. Continuous scan from the second to the ninth images presented in Fig. 2e shows that bubble growth led to the formation of a gas slug. This is rather similar to the situation presented in Fig. 2d. However, it is clearly seen from the remaining images (starting from the 10th) in Fig. 2e that this gas slug rose up when it became large enough. The recorded movies show that this translation of the gas slugs within the triangular channel was periodic. The peculiar behavior can be explained as follows. For triangular channels, the liquid phase always occupies the channel corners owing to the capillary force or the Gregorig effect (Carey, 1992), implying that a continuous liquid phase can be maintained although the gas phase occupies the majority of the cross-section of the channel. Thus, the buoyancy force always exists and it gets stronger with the growth of the gas slug. Consequently, the up-motion of the elongated bubble in the miniature triangular channel can be maintained, i.e., the drift velocity is not zero for a miniature triangular channel. The bubble behaviors for the other two miniature triangular channels were generally similar to the scenario displayed in Fig. 2e. It was found, however, that as the channels' size was reduced, the gas slugs in the triangular channels became longer and the rising velocity smaller.

The bubble behaviors in the miniature square and rectangular channels are presented in Fig. 2f and 2g. It is seen that the scenario of the bubble behaviors in these miniature channels are generally similar to those in the miniature triangular channel, i.e., the drift velocity is not zero even though the elongated bubble seems larger than that in the triangular channel.

4. Drift velocity for mini channels

As mentioned earlier, the drift velocity of gas slugs in a large round tube is proportional to the square root of the tube diameter. In the existing literature, it is generally agreed that the following simple equation can be used to predict the drift velocity for a low viscosity liquid in

a large round tube (Wallis, 1969):

$$V_b = 0.35\sqrt{gd} \tag{3}$$

For small-diameter circular tubes, Eq. (3) may not be applicable because the effect of the surface tension on the bubble behaviors in small tubes becomes relatively important. By considering this effect, Tung and Parlange (1976) obtained the following equation for predicting drift velocity in a small tube:

$$V_b^2/gd = 0.272 - 0.472\sigma/\rho gd^2 \tag{4}$$

Note that the last term in the right-hand side of Eq. (4) represents the relative importance between the surface tension and the buoyancy force. As will be shown, however, Eq. (4) is not applicable for predicting the drift velocity in the miniature noncircular tubes tested in the present work.

We now present the measured drift velocities in mini channels. To this end, we first need to determine the rising velocity of gas slugs in a tube with a given cross-sectional shape and size. As presented earlier in Fig. 2, the gas slugs behaved periodically in the tubes; and thus, the

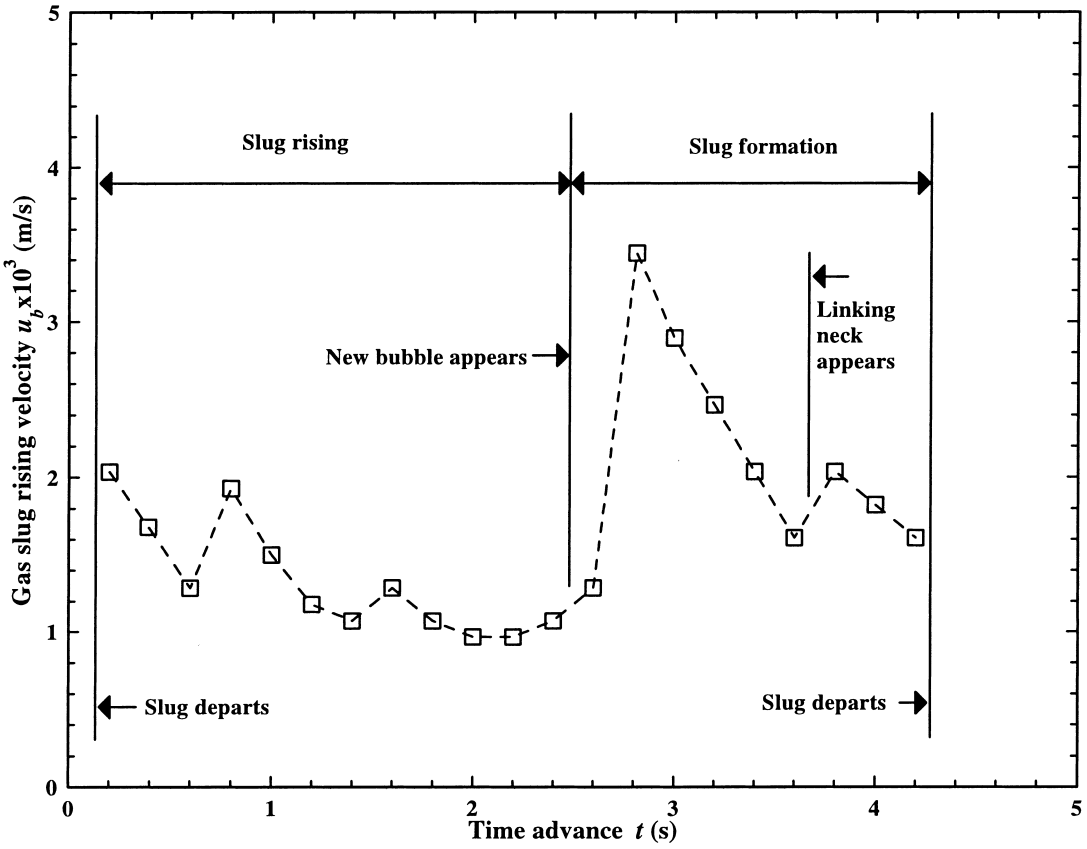

Fig. 3. Time dependent slug rising velocity.

bubble velocity varied with time accordingly. Fig. 3 displays a typical variation of the bubble velocity for the 1.5 mm-square channel with time. It is seen from this figure that the bubble velocity fluctuated significantly during the period of slug formation and rising. As shown, the bubble behaviors in the channel can largely be divided into two stages: the stage of the slug rising and the stage of the new slug formation. During the first stage, slug departed from the nozzle and rose upward relatively steadily. The fluctuation of the rising velocity during this stage was due to the fact that the slug experienced a deformation process after it departed from the nozzle by overcoming the surface tension between the slug and the nozzle. During the second stage, a new bubble appeared and slug formation started. The slug rising velocity fluctuated greatly when the bubble rushed out of the nozzle, after the gas pressure inside the nozzle got accumulated high enough. The second peak took place when the linking neck appeared between the slug and the nozzle. Therefore, during this stage the rising velocity was influenced by the newly-formed slug. In view of the aforementioned behaviors, the determination of the slug drift velocity should be based on the first stage and the influence of the second stage should be excluded. Accordingly, the slug drift velocity can be obtained from the average value of the slug rising velocity over the first stage. It should be pointed out that

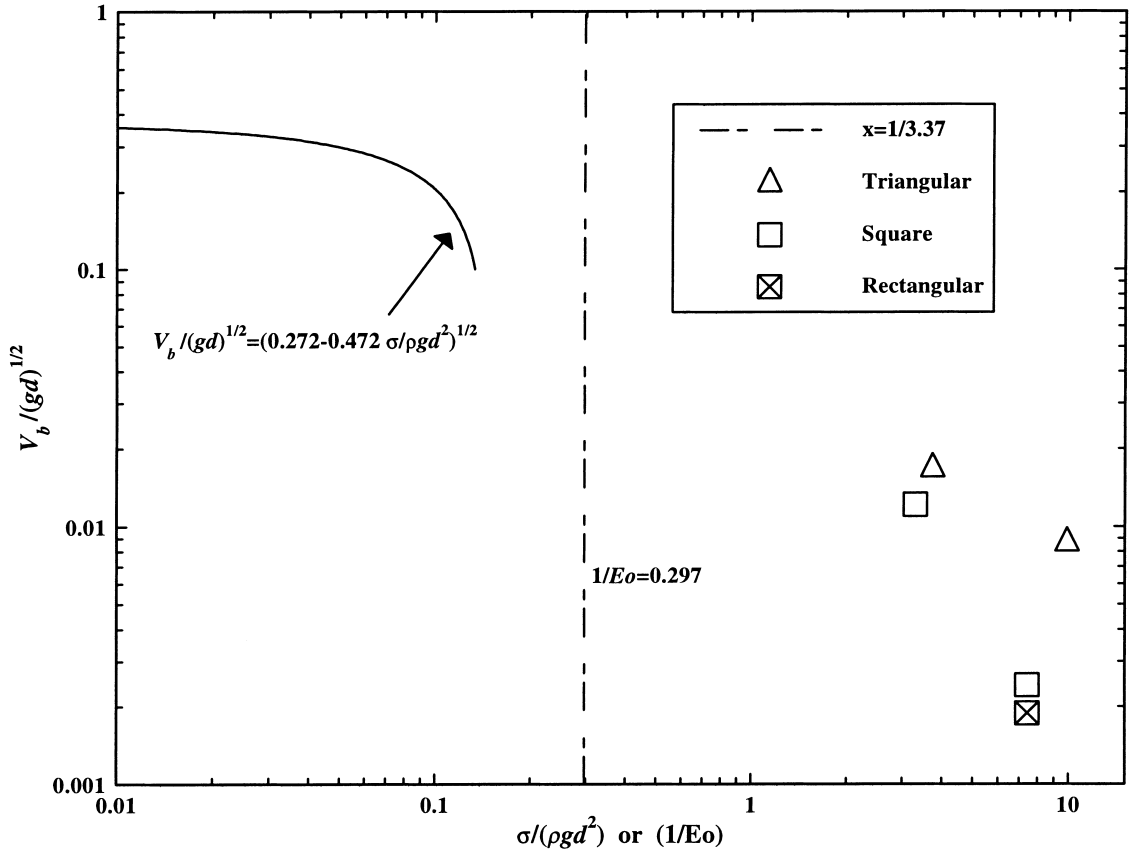

Fig. 4. Slug rising velocities in miniature noncircular channels.

the present detailed observation of the slug formation and rising behaviors has never been addressed in the existing literature.

Fig. 4 presents the gas slug rising velocities in the triangular, square, and rectangular channels tested in the present work, in terms of the Froude number $Fr = V_b/(gd)^{1/2}$ and the reciprocal of the Eötvös number $1/Eo(Eo = \rho g d^2/\rho)$. For comparison, Eq. (4) (represented by the solid line) is also plotted in Fig. 4. In addition, the dashed line ($1/Eo = 0.297$ or $Eo = 3.37$) in Fig. 4 implies that the surface tension becomes dominant, such that the gas slug velocity in a circular tube becomes zero for, $1/Eo > 0.297$ (Wallis, 1969). It is clear from Fig. 4 that the previous studies (Zukoski, 1966; Tung and Parlange, 1976; Kataoka et al., 1987) have focused on the bubble rising velocity in circular tubes for the range of $1/Eo < 0.297$, whereas the present study primarily concerns the bubble behaviors in the miniature noncircular tubes in the range of $1/Eo > 0.297$. Another important observation from Fig. 4 is that the bubble rising velocity in a circular tube will be taken to be zero if $1/Eo \geq 0.297$. However, for noncircular tubes, the experimental data shows that the bubble rising velocity is not zero even though the reciprocal of the Eötvös number $1/Eo$ is much larger than 0.297. Furthermore, it is found from Fig. 4 that the bubble rising velocities in the triangular and the square tubes became smaller with the decrease of the channel size or with the increase of $1/Eo$. This trend is similar to that for the circular tubes as represented by the solid line [Eq. (4)] in Fig. 4. To predict the bubble rising velocity in the noncircular channels in the range of $1/Eo \geq 0.297$, a new theory needs to be developed.

5. Concluding remarks

The bubble behaviors in vertical miniature circular and noncircular (triangular, square and rectangular) tubes closed at the bottom and filled with stagnant water have been visually studied. The experimental results show that for large circular tubes ($d > 2.9$ mm), bubbles rose up periodically. As the diameter of the circular tubes became smaller, the up-motion of the gas slugs was slowed down, and ceased completely when the tube size was sufficiently reduced ($d \leq 2.9$ mm). For the miniature triangular channels, however, it is found that the gas slug always rose upward even though the hydraulic diameter was as small as 0.866 mm. Similarly, it has been found that the drift velocity in the other two kinds of polygonal (square and rectangular) channels is not zero. One of the most important implications of the unusual behavior is that when a polygonal-cross-sectional channel and a circular tube are filled with a stagnant liquid and subjected to a heating load, the critical heat flux for the former one will be higher than that for the latter one. This is simply because the generated bubble in the polygonal channel would automatically move up due to the existence of the buoyancy force. However, for the miniature circular tube, the growth of the bubbles generated in the tube would cause the liquid phase to be discontinuous and as a result, the buoyancy force vanishes, leading to a partial dryout within the channel.

Acknowledgements

This work was supported by a Hong Kong RGC Earmarked Research Grants No. HKUST 6045/97E.

References

Benjamin, T.B., 1968. Gravity currents and related phenomena. Journal of Fluid Mechanics 31, 209–248.

Carey, V.P., 1992. Liquid–vapor Phase-change Phenomena. Hemisphere, New York.

Guntly L.A., Costello, N.F., 1991. Condenser with small hydraulic diameter flow path. US Patent 4998580.

Kataoka, Y., Suzuki, H., Murase, M., 1987. Drift-flux parameters for upward gas flow in stagnant liquid. Journal of Nuclear Science & Technology 24, 580–586.

Tung, K.W., Parlange, J.Y., 1976. Note on the motion of long bubbles in closed tube-influence of surface tension. Acta Mechanica 24, 313–317.

Wallis, G.B., 1969. One Dimensional Two-phase Flow. McGraw-Hill, New York.

Zukoski, E.E., 1966. Influence of viscosity, surface tension, and inclination angle on motion of long bubbles in closed tubes. Journal of Fluid Mechanics 25, 821–837.